Precipitation Efficiency of Warm-Season Midwestern Mesoscale Convective Systems

PATRICK MARKET AND STACY ALLEN*

Department of Atmospheric Science, University of Missouri—Columbia, Columbia, Missouri

RODERICK SCOFIELD, ROBERT KULIGOWSKI, AND ARNOLD GRUBER

NOAA/NESDIS/Office of Research and Applications, Camp Springs, Maryland

16 July 2002 and 23 April 2003

ABSTRACT

The precipitation efficiencies for mesoscale convective systems (MCS) over the central United States are calculated. During July–September 2000 and June–September 2001, 24 MCS for which sufficient data were available occurred over or near Missouri. Precipitable water fields from the hourly Rapid Update Cycle (RUC) and radar-derived precipitation grids are used to calculate the precipitation efficiency. Geostationary Operational Environmental Satellite soundings and RUC winds are used to assess the pre-MCS environment. Statistical analysis reveals that precipitation efficiency has a relatively strong positive correlation with the relative humidity in the layer between the surface and the lifting condensation level; significant negative correlations are found between the precipitation efficiency and both the convective inhibition and the environmental wind shear. The latter, inverse relationship between shear and precipitation efficiency supports the findings of previous investigators.

1. Introduction

The precipitation efficiency (PE) of various rain and snow systems has been a topic of serious scientific inquiry beginning with Braham (1952), who completed the water budget for a convective system observed during the Thunderstorm Project. In the intervening years, PE has been evaluated for both warm-season (e.g., Auer and Marwitz 1968; Fankhauser 1988) and cold-season (Hindman et al. 1981; Szeto et al. 1997) systems. However, the historical emphasis has tended toward a more thorough understanding of deep moist convection. Recent activity in this arena has focused on the numerical modeling of tropical and midlatitude convection (e.g., Doswell et al. 1996; Li et al. 2002).

During this period, the efficiency with which precipitation systems process moisture has remained largely an academic pursuit. The precipitation efficiency of a rain or snow system can best be determined as a time average over its lifetime (Doswell et al. 1996). This approach demands an analysis a posteriori, and so the value of PE as a *prediction* tool would seem nonexistent. One method for approximating the precipitation efficiency has been developed by Scofield et al. (2000) and has performed well as a component for estimating convective precipitation. Known as the ''moisture correction factor,'' it is the product of the precipitable water (PW) and the surface-to-500-hPa mean relative humidity (RH), factors which are important in the generation of convective rainfall.

The goal of the current work is to improve PE estimation in order to highlight regions of flash-flood potential up to 6 h in advance using variables derived largely from Geostationary Operational Environmental Satellite (GOES) soundings. Consider two columns of large but equal precipitable water. If convection occurs in both columns, the one with the higher PE is likely to generate greater rainfall totals. As such, the PE is calculated for a number of Midwestern mesoscale convective systems (MCS), and GOES sounding profiles from the precursor environment of Midwestern MCS are analyzed to determine whether a predictive equation for PE might be determined. This note is organized as follows: In section 2 we examine the literature on PE studies, in section 3 we detail the data used for the study

* Current affiliation: Premier Marketing Group, Columbia, Missouri.

Corresponding author address: Patrick S. Market, Dept. of Atmospheric Science, University of Missouri—Columbia, 387 McReynolds Hall, Columbia, MO 65211.
E-mail: marketp@missouri.edu

and our method of calculating PE, in section 4 we discuss the statistical link between PE and several controlling environmental variables, and in section 5 we offer some concluding remarks.

2. Background

Although the history of precipitation-efficiency studies is long (e.g., Braham 1952; Li et al. 2002) and covers both observational (e.g., Marwitz 1972; Heymsfield and Schotz 1985) and modeling studies (e.g., Lipps and Hemler 1986; Ferrier et al. 1996), few studies have statistically demonstrated the physical controls on PE. With this work, we intend to add value to the current knowledge of PE discussed by Lamb (2001) so that operational forecasters can predict MCS precipitation efficiency.

Braham (1952) worked with airflow and moisture budgets of typical airmass thunderstorms studied during the Thunderstorm Project. Surface observations and soundings provided sufficient data to calculate average moisture budgets, showing that total inflow of water vapor into these thunderstorms was almost 9 times the amount of precipitation measured at the ground. These numbers translate to around 10% PE, but it was Newton (1966) who did the efficiency calculation from Braham's (1952) values. Newton (1966) also found that squall-line PE averaged near 50%, as much as 5 times more efficient at removing moisture from the atmosphere than the airmass thunderstorms of Braham (1952). Newton (1966) theorized that higher efficiencies were achieved by 1) minimizing the amount of cloud contact with unsaturated air, thereby preventing evaporative losses from dry-air entrainment, 2) the longer lifetimes of squall lines versus airmass thunderstorms, and 3) greater pressure perturbations associated with storms of a more dynamical nature. These two works represent some of the earliest quantitative studies to address how water vapor is redistributed within and by storms. In this same period, Sellers (1965) explored PE as a climatological value, dividing the accumulated precipitation by PW to establish those regions more prone to rain or snow over extended periods.

Advances in observational data sources, especially the introduction of radar, allowed for finescale estimates of updraft water uptake and of precipitation. Auer and Marwitz (1968) studied 18 hailstorms to determine quantitative air and moisture fluxes along with precipitation efficiencies. The definition of PE used in their study is the ratio of surface precipitation rate estimated by radar to moisture convergence rate at the 800-hPa flight level. This level captures moisture intake at the cloud base because of the storm's updraft, the main source for water in the cloud. Eight calculated efficiency values ranged from a low of 21% to a high of 120%, with fully one-half of the values falling between 50% and 60%. Although these are storm total PEs, efficiencies of over 100% were obtained in part because of underestimates of inflow during periods with little updraft moisture intake and high rainfall rates. Marwitz (1972) continued the work of Auer and Marwitz (1968) and created a larger dataset with which to test a postulated correlation between wind shear and PE. In physical terms, Marwitz (1972) argued that strong wind shear acts to decrease PE by entraining dry air into storms, causing evaporation of potential precipitation. Marwitz's (1972) analysis (his Fig. 1) shows a negative correlation between the variables and stands as one of the first works to attempt a statistical explanation for PE magnitude.

One of the most thorough studies of thunderstorm precipitation efficiency is detailed in Fankhauser (1988). Data from seven storms observed during the Cooperative Convective Precipitation Experiment (CCOPE) were obtained using aircraft, radar histories, rawinsondes, and surface mesonetwork stations; the values for the seven storms of interest ranged from 19% to 47%. These values are physically realistic (0%–100%), and so Fankhauser (1988) went beyond simply calculating PE and attempted statistical correlations of greater breadth than Marwitz (1972). Various environmental quantities were considered as determining factors of PE. The kinetic energy as measured by low-level wind speeds showed a significant positive correlation. Increasing cloud-base area and cloud-base mixing ratio increased PE, and lowering cloud-base heights increased PE. What was most surprising was the lack of significant correlation with variables assumed to be of strong influence on PE. Bulk Richardson number, which is the ratio of buoyant energy to wind shear and can give clues to storm organization, did not correlate well with PE, and neither did convective available potential energy (CAPE), a measure of potential updraft strength. A plot of wind shear versus PE as in Marwitz (1972) did not support an inverse relationship, most likely because for low shear values and small datasets the scatter about the line is too great to show any relationship. As a comprehensive observational study, Fankhauser (1988) provided some of the most detailed PE work to date and yet showed that more statistical analyses are needed to help to understand the factors controlling PE.

Doswell et al. (1996) treated the subject of flash flooding by breaking the topic into several key components. Precipitation efficiency was discussed because of its influence on instantaneous rainfall rate and storm total precipitation. They defined PE as the ratio of water mass falling as precipitation to the influx of water vapor mass into the cloud. To determine these two masses, Doswell et al. (1996) suggested that defining a volume around the system of interest and employing winds relative to the moving system would facilitate influx and precipitation calculations. They also stated that these two quantities are most meaningful when averaged over the lifetime of a system because instantaneous values have great variation. As depicted in Fig. 1, efficiency begins at 0% when moist inflow is large but no rain is yet falling, increases to between 0% and 100% as precip-

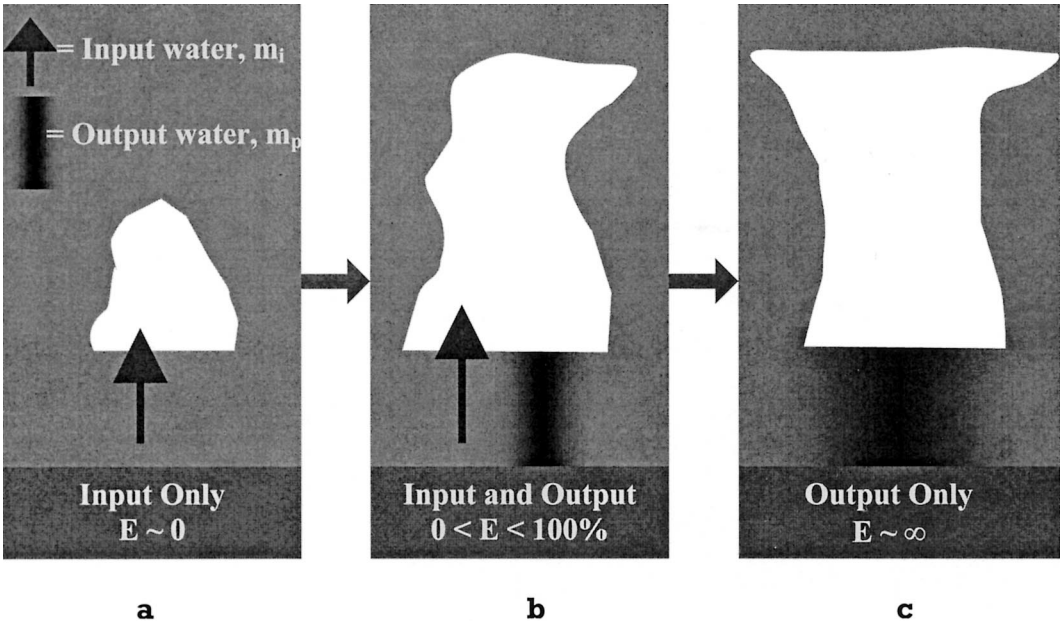

FIG. 1. The instantaneous variation of precipitation efficiency (E) with storm stage: (a) initiation when moisture inflow (m_i) is taking place—a cloud has formed but no rain is reaching the ground ($E \sim 0$); (b) mature stage when inflow persists while rain (m_p) is reaching the ground ($0\% < E < 100\%$); (c) dissipating stage when inflow has ceased yet rain is still reaching the ground ($E \sim \infty$).

itation falls and inflow continues, and then becomes infinite during the dissipating stage when precipitation cuts off all inflow. Thus, one may assume that system-average PE is dependent on various observable environmental factors such as relative humidity and wind shear. Although little treatment was given by Doswell et al. (1996) to those factors that control PE, their well-rounded discussion of PE as it relates to flash flooding provided further impetus for attempting to develop a method to predict PE.

A summary of the precipitation-efficiency values derived from previous studies is provided in Table 1. To date, most investigators have relied upon observed data, although modeling efforts have been undertaken lately to arrive at values for the calculation of PE. Another recent trend involves studies of precipitation systems other than midlatitude, continental convection. Both the high latitudes and the Tropics have borne precipitation systems whose precipitation efficiencies have been evaluated; the high-latitude systems have had meso-α to synoptic-scale features; several of the tropical studies revolve around maritime weather systems.

Of interest, too, are the methods by which previous investigators arrived at their PE values. Most authors employed some version of the precipitation-to-ingested-moisture ratio, which dominated the early literature. Recent studies (e.g., Gamache and Houze 1983; Chong and Hauser 1989; Li et al. 2002) have made use of a more elaborate approach, based upon an actual budget expression, that also accounts for processes such as evaporation. Last, there is the unique approach of Rauber et al. (1996), who evaluated the PE as the ratio of the latent heat put into the atmosphere by precipitation production to the ocean surface heat flux. Note that all studies that clearly identified their PE as a ratio of time-mean or integrated values for precipitation and ingested moisture found PE values of less than 100%. Such a range of average values fits well with the assertion of Doswell et al. (1996) that a time-mean PE is more physically meaningful than instantaneous values, which may range from zero early in the life cycle of a convective system (exclusively inflow and updraft) to infinity as the system is decaying (exclusively precipitation and downdraft).

3. Method

A first step in this work is to calculate the PE of individual MCS across our area of interest (Fig. 2). Choosing a method of calculating PE that would be easily reproducible given data currently available within the meteorological community is a primary goal. Indeed, even in the absence of detailed aircraft data or sufficient time to calculate a complete water budget, a means of estimating the PE in a real-time operational environment is still possible. An example is the Sellers (1965) method (hereinafter called the Sellers method) of calculating PE, which is ideally suited to the data available for this study. The Sellers method defines PE climatologically as the ratio of mean daily precipitation to the average precipitable water of a given location; this approach is a departure from much of the preceding

TABLE 1. Investigations that involved precipitation efficiency, along with the type of system studied, the type of data source employed to calculate the efficiency, and the values found. For those studies that involve multiple precipitation systems, the range of calculated values is shown.

Author	Type of system	Obs or modeled	PE value
Braham (1952)[a]	Midlat thunderstorm	Obs	10%
Sellers (1965)	Climatological	Obs	5%–19%
Newton (1966)	Midlat squall line	Obs	50%
Fankhauser (1966)	Midlat thunderstorm	Obs	60%
Auer and Marwitz (1968)	Midlat hailstorms	Obs	21%–120%
Chisholm (1968)	Midlat thunderstorm	Obs	21%
Hartzell (1969)	Midlat hailstorm	Obs	45%
Chisholm (1970)[b]	Midlat squall line	Obs	~100%
Marwitz (1972)	Midlat hailstorm	Obs	~4%
Foote and Fankhauser (1973)	Midlat hailstorm	Obs	15%
Chalon et al. (1976)	Midlat hailstorm	Obs	40%
Houze et al. (1976)[c]	Midlat frontal system	Obs	60%–90%
Caracena et al. (1979)	Midlat thunderstorm	Obs	85%
Hobbs et al. (1980)	Midlat cyclone	Obs	40%–50% WS[d] 20%–50% CS[d]
Hindman et al. (1981)	Midlat winter mountain storms	Obs	7%–49%
Carbone (1982)	Midlat cold front	Obs	70%
Gamache and Houze (1983)	Tropical MCS	Obs	~59%
Heymsfield and Schotz (1985)	Midlat squall line	Obs	25%–40%
Lipps and Hemler (1986)	Tropical convection	Mod	~40%
Fankhauser (1988)	Midlat thunderstorms	Obs	19%–47%
Ryan et al. (1989)[c]	Midlat cold front	Obs	0%
Cotton et al. (1989)	Midlat Mesoscale convective complex	Obs (composite)	49%–113%
Chong and Hauser (1989)	Tropical squall line	Obs	45%–57%
McBean and Stewart (1991)[e]	Midlat frontal system	Obs	70%
Ferrier et al. (1996)	Tropical and midlat squall lines	Mod	24%–45%
Rauber et al. (1996)	Tropical convection	Obs	20%–30%
Szeto et al. (1997)	High-lat frontal system	Mod	0%–80%
Hanesiak et al. (1997)	High-lat warm front	Obs	60%
Li et al. (2002)	Tropical convecton	Mod	20%–130%

[a] Derived from Newton (1966, p. 711).
[b] Derived from Marwitz (1972, p. 369).
[c] Derived from Heymsfield and Schotz (1985, p. 1585).
[d] WS denotes warm-sector systems; CS denotes cold-sector systems.
[e] Derived from Hanesiak et al. (1997, p. 1564).

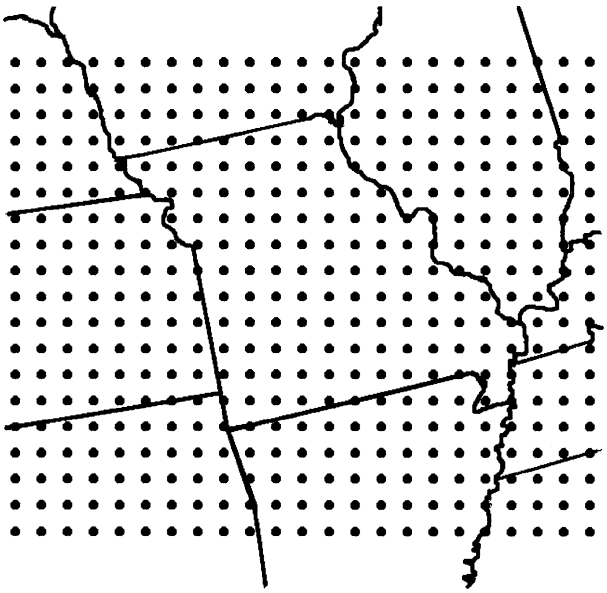

FIG. 2. The grid area used, and the points at which precipitation and precipitable water were calculated.

literature. Most previous studies make use of finescale, research-quality data to calculate a moisture flux divergence and use that value in place of precipitable water as an ingested moisture variable.

For this study of mesoscale features, it is necessary to scale down the time interval to capture the life cycle of MCS. The 6-h total precipitation amounts available from stage-III radar mosaic estimates (Fulton et al. 1998) lent themselves well to this study. The accumulated 6-h periods often capture the formation, maturity, and dissipation of an entire MCS life cycle. Although a climatological approach originally, the statistical basis of the Sellers method also lent itself to the datasets available for this study. Because time averaging of both precipitation and precipitable water became necessary (discussed later), the Sellers approach was all the more attractive. Again, a time-average PE is often more revealing than an instantaneous value.

It is true that the Sellers approach deviates from the more common ratio of precipitation to *ingested* moisture by forming a ratio with the *available* moisture in the denominator. There is no accounting for system-relative

inflow or how much moisture may be converging into a given column; efficiency is determined using the moisture present and not its time rate of change. In the context of the more common ratio, the Sellers approach assumes that all of the PW is lifted in a convective column. However, our application of the Sellers approach (discussed shortly) spans the lifetime of each MCS studied, yielding a mean PE for each system. On a practical level, the technique is one that may be employed easily in real time. Moreover, the available moisture, as represented by the PW, is the outcome of a single vertical integration. Not only does the calculation of moisture flux divergence require additional u and v wind fields, but also derivatives involving those quantities enhance the opportunities for error in the final PE calculation.

a. Data

The two terms in the Sellers definition of PE require precipitation data and precipitable water for our area of interest. The numerator of the Sellers method requires an accumulated precipitation depth. Grids of precipitation depth, in millimeters, accumulated over 6-h periods ending at 0000, 0600, 1200, and 1800 UTC, are archived for summertime MCS cases. The stage-III radar mosaic is created on a roughly 4-km square grid from combined radar ranges across our area of interest. Precipitation amounts are derived based on either the average of overlapping grid box values or on the single radar-sampled box value. Rain gauge networks are used to quality check the precipitation values reported by radar measurement as well as to compute mean-field corrections (Fulton et al. 1998).

The denominator of the Sellers PE definition requires computation of average PW. To determine average precipitable water during the corresponding 6-h time period as precipitation depth, it became necessary to track PW with the motion of the MCS. To do this, Rapid Update Cycle (RUC) Model initialization output is used to calculate PW for the area of our grid for each hour in the 6-h period. One disadvantage of PW is that it measures the water vapor content of an entire column of atmosphere, whereas essentially only the low-level moisture is available to the storm. However, the amount of vapor available at higher levels is negligible because of the low temperature and corresponding low moisture content of the less dense air. PW approximates the amount of low-level moisture available to the system, although some of the vapor it measures *is* located above the inflow region and is generally not ingested by the system.

The last major data source is the GOES soundings. To create a predictive equation for PE based on GOES sounding parameters, hourly GOES soundings covering our grid that contain vertical profiles of temperature and dewpoint were collected. Winds obtained from RUC initialization hours for levels corresponding to those of GOES temperature and moisture provide kinematic detail. Major improvements in GOES technology occurred following the launch of GOES-I (*GOES-8*) in the mid-1990s (Menzel and Purdom 1994). Sounding operations are vastly improved by separating them from imaging functions and by increasing sensitivity. Temperature and moisture profiles are now derived for areas covering both oceans and landmasses that are not contaminated by cloudiness. These new sounders fill the gaps of the traditional rawinsonde network, whether soundings are made over data-sparse oceans, areas within the network that need additional coverage, or at times between traditional balloon launches (Menzel et al. 1998). Examples of the value of derived sounding products in real time can be found in Kadin and Kusselson (2000). With the expanding array of GOES sounder products available online, the Forecast Products Development Team Web site provides many new datasets offered by the Office of Research and Applications (ORA) at the National Environmental Satellite, Data, and Information Service (NESDIS). For this study, vertical sounding profile images and raw data files were archived from the many locations available that cover our area of interest for as many hours prior to convection as possible.

This research makes use of vertical atmospheric profiles from both the RUC initial fields and the GOES sounder, and one may question the validity of the information they provide. Thompson and Edwards (2000) compared a modest sample of RUC Model soundings to observed soundings in a supercell environment and found the former to be ''reasonably representative'' of actual profiles. However, they did find that the RUC dewpoints at the surface and 850 hPa were generally 1°–2°C too dry, which would cause an underestimate of the precipitable water in the typical grid column used in this study. The current study also employs RUC winds to calculate vertical shear profiles in the MCS precursor environment. With the Thompson and Edwards (2000) dataset, the mean error for the 0–6-km shear vector magnitude was -0.6 m s^{-1}, with a mean absolute error of 3.0 m s^{-1}.

Dostalek and Schmit (2001) performed an in-depth comparison of GOES-retrieved profiles to radiosonde observations. Their comparisons for the summer season for 0000 UTC (which typifies the bulk of the soundings used in this study) radiosonde flights revealed a high degree of correlation between the remotely sensed and in situ profiles. For a sample size of 1327 observations, Dostalek and Schmit (2001) found a mean total precipitable water (TPW) from the radiosonde flight of 29.5 mm, with a standard deviation of 4.6 mm, and a bias in the GOES TPW of only -0.2 mm. Although the relationship between the GOES and radiosonde TPW values for summer 0000 UTC pairs exhibited the lowest of the eight (all four seasons at both 0000 and 1200 UTC) calculated correlation coefficients ($r = 0.91$), it is nonetheless robust.

b. PE calculation

Before computing PE, the 4-km precipitation grids must be rescaled to make them compatible with the 40-km grid scale of the RUC PW. This is accomplished by averaging 10 × 10 clusters of adjoining grid boxes to produce a precipitation grid of 40-km grid spacing. Because precipitable water is found at each hour and precipitation depth should be temporally the same (but is a 6-h accumulation), we assume that the precipitation is evenly distributed across the 6-h period and so divide each grid point value by 6. The output is an hourly area-average precipitation depth in millimeters. We note that this method can lead to large underestimates in the hourly precipitation, especially in the case of a rapidly moving MCS (to be further discussed later). Precipitable water, as derived from RUC hourly initializations, is on a slightly larger grid, with different reference points than our precipitation grid. Grid bilinear interpolation is used to match up the two different grids point to point, and maps of hourly PW for our area of interest are produced.

From hourly radar summaries over the central United States, the area on which an MCS precipitates at the top of the hour is outlined on a numbered grid template for each hour within the 6-h period. These images are not based on the 6-hourly stage-III totals but are hourly radar summaries available online from the National Climatic Data Center (http://lwf.ncdc.noaa.gov/oa/radar/radardata.html). From these outlined grids, the hourly areal extent of the MCS is determined. The corresponding grid points are added to find the total of hourly average precipitation and PW of the MCS environment for that hour. This summation is done for all hours within the period to obtain a 6-h total of precipitation depth (in millimeters) and precipitable water (in millimeters) processed by the MCS. According to the Sellers PE definition, precipitable water should be an average value over the same time period as the total precipitation. To obtain a 6-h average PW value, the total PW is divided by 6 before the final PE calculation is completed. An outline of the procedure that addresses the numerator and denominator of the Sellers PE definition is given in Fig. 3.

To summarize, the approach is quantified as a ratio of precipitation P to ingested moisture Q, with

$$P = \sum_{i=1}^{6} \left(\frac{R}{6}\right)_{g(i)} \quad \text{and} \tag{1}$$

$$Q = \frac{\sum_{i=1}^{6} (\mathrm{PW}_i)_{g(i)}}{6}, \tag{2}$$

where R in (1) is the total 6-h precipitation amount from the stage-III mosaics, PW_i is the hourly precipitable water from the RUC, and the subscript $g(i)$ signifies the grid points affected by precipitation. To find the final hourly average PE, the ratio of the numerator (the total of hourly average precipitation depths) to the denominator (hourly average precipitable water depth) is computed and multiplied by 100.

c. Sounding choice

After calculating precipitation efficiency, a GOES sounding must be chosen so that environmental variables can be correlated with the PE value found. Chosen soundings are representative of the environment into which an MCS will move or develop and provide information about low-level moisture content, midlevel lapse rates, and environmental wind shear. For each period with a calculated PE, a sounding near the MCS formation location or in the path of a mobile MCS is chosen for an hour early in the period or 1 or 2 h before the beginning of the period. The earlier a sounding is chosen the more likely a proximity sounding will be available, because a less developed MCS will have a smaller shield of cirrus clouds that may obscure potential GOES soundings. Another reason for choosing soundings early in the period is to avoid MCS that alter their environments via cold low-level outflow. After considering these factors, soundings are chosen to enable calculation of precursor environmental variables that influence PE.

4. Results

a. Evaluation of PE values

Before beginning steps to create a predictive equation for PE, the validity of this newly applied PE calculation method must be established. Because other PE calculation methods have provided consistency throughout the years, calculating with a method originally proven only in climate studies requires intercomparison to ensure that the method is valid. Values from 2000 and 2001 cases range from a minimum of 4% PE to a maximum of 48% PE, which is consistent with the preponderance of the literature (see Table 1). Yet, that PE values in this study average near 25% may indicate that the Sellers method yields values somewhat lower than those of other methods and further suggests a systematic error, especially in light of the aforementioned dry bias in the RUC-derived PW values. One possible contribution to the low values obtained in this study is described below.

By assuming that the 6-h accumulated precipitation fell equally among all 6 h, we neglect the fact that some points received all of their precipitation in 1 or 2 h and not 6. This assumption tends to decrease the total precipitation accounted for in the Sellers PE numerator, causing the PE percentage to decrease. This is especially true for cases of fast-moving MCSs because they can drop significant rainfall in a short time. For example, one grid point may receive 6 in. (1 in. = 2.54 cm) of rain in 1 h (an extreme rainfall) and no rain in the other

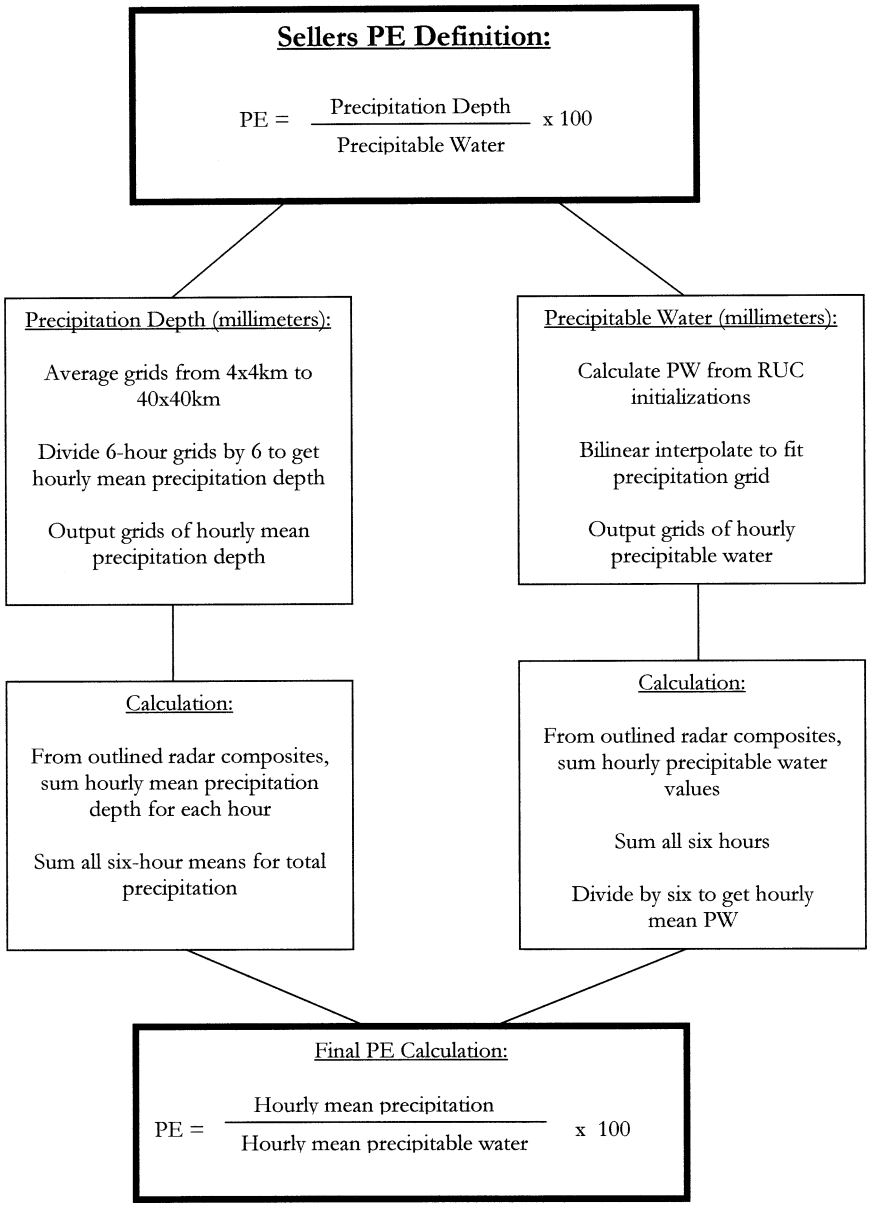

FIG. 3. Flowchart illustrating the steps performed to calculate Sellers precipitation efficiency given the data used in this study.

5 h because the MCS has moved out of the area. Our average method divides the total precipitation by 6, giving an average rainfall of 1 in. h^{-1}. Therefore, when summing the hourly rainfall contributions from our outlined MCS areas, only 1 of the total 6 in. that fell is accounted for because for only 1 h did the MCS precipitate on that grid point.

In this way, a fast-moving MCS will have diminished PE and a slow-moving MCS will be more accurately represented. Analysis of the thirty-four 6-h periods for which PE was calculated reveals that the median period during which rain actually fell on a grid point was 2.5 h, suggesting that only 42% of the accumulated precipitation is accounted for in the typical PE calculation. As a consequence, the equation tends to predict lower PE values. However, the Sellers PE calculation method discriminates between high and low (48% versus 4% PE), which can be useful to forecasters looking for the most critical precipitation systems.

b. Development of predictive PE equations

The GOES soundings chosen to be representative of the MCS environment for the 2000 summer season are used both in performing single correlations and in creating a predictive equation. The dataset includes twenty

TABLE 2. Variables with and without significance from 2000 cases. Correlation coefficients and confidence intervals are provided. Here, θ_e is equivalent potential temperature.

Variable	Correlation coef	Confidence interval
Surface-to-LCL relative humidity	0.392	90%
CIN based on lowest 100-hPa parcel	−0.481	95%
Cloud shear over warm-cloud depth	−0.384	90%
CAPE based on lowest 100-hPa parcel	0.121	30%
CIN based on maximum θ_e parcel	0.062	20%
Precipitable water	−0.019	5%
Warm cloud depth	0.167	50%
Warm-cloud-depth relative humidity	−0.069	30%

6-h periods and their corresponding soundings. First, temperature and moisture profiles from the chosen soundings are put into an analysis program developed originally by Moore and Pino (1990). The output variables calculated by the program include various stability indices such as the Showalter and total totals, parcel-method quantities based on different initial parcel levels such as the level of free convection and equilibrium level, moisture parameters such as surface-layer gradients of specific humidity and mixing ratio, and wind shears over various atmospheric depths.

Variables derived from the GOES soundings are put into a statistical program for a simple, linear correlation with PE. Of the correlation coefficients obtained, the quantities having coefficients greater than 0.35 or less than −0.35 are found to be statistically significant (confidence interval > 90%) and are outlined in Table 2. In addition, some quantities that are expected to have a strong physical relationship to PE but correlated poorly in the test data are also listed in Table 2. All quantities listed are output from the Moore and Pino (1990) program, meaning no variables directly listed from the GOES sounder had significant correlation with the calculated PE.

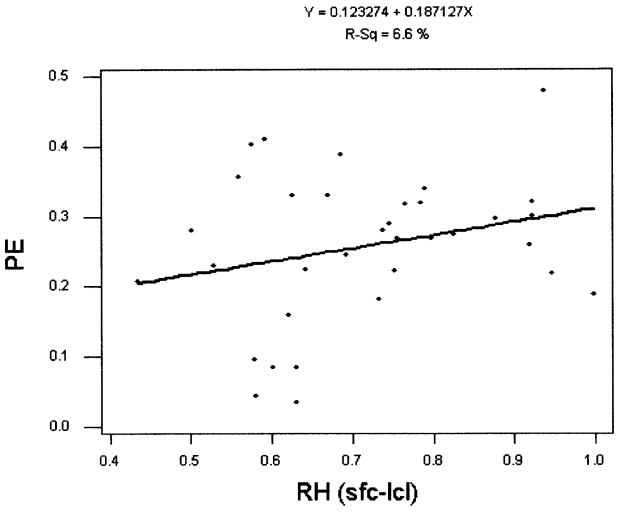

FIG. 4. Scatterplot of PE (in decimal form) vs the mean surface-to-LCL relative humidity (in decimal form) from data for 2000 and 2001 (N = 34).

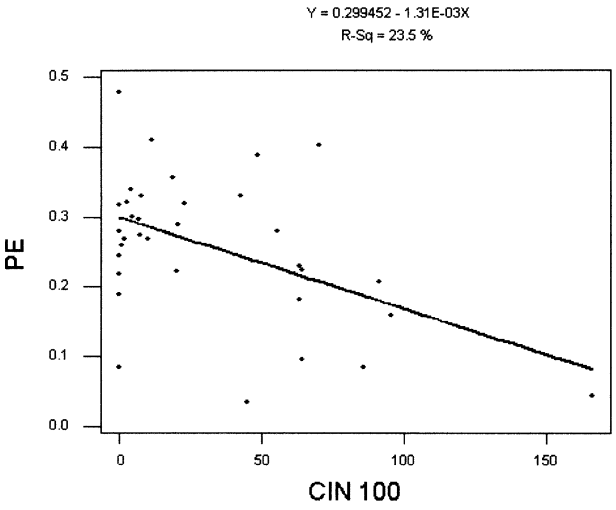

FIG. 5. Scatterplot of PE (in decimal form) vs CIN (J kg^{-1}) from data for 2000 and 2001 (N = 34).

In addition to the single correlations, linear regressions are shown for the three best individual correlates, which are defined in detail below. These plots are enhanced by data from 2000 and 2001 (number of samples N = 34). Each shows a linear relationship, and the slope of the line indicates either a direct (positive slope) or inverse relationship (negative slope). The relative humidity in the surface-to-lifting-condensation-level (LCL) layer (Fig. 4) exhibits a weak positive correlation with PE; the convective inhibition (CIN) of a parcel from the lowest 100 hPa (Fig. 5) and the bulk shear over the warm cloud depth (from the cloud base to the level at which the cloud temperature becomes 0° C; Fig. 6) show more robust inverse relationships with PE.

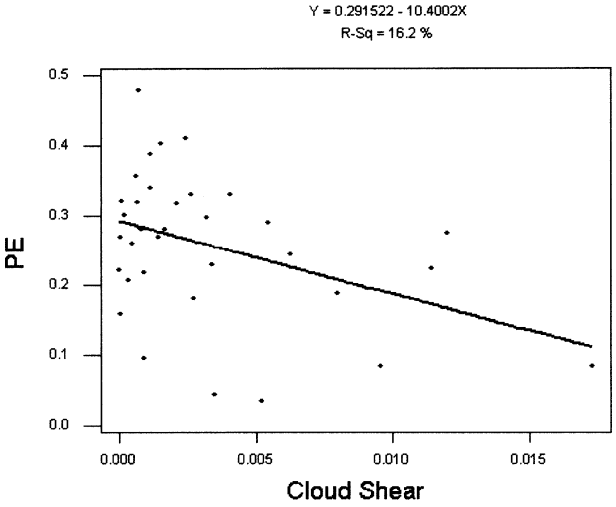

FIG. 6. Scatterplot of PE (in decimal form) vs shear over the warm cloud depth (s^{-1}) from data for 2000 and 2001 (N = 34).

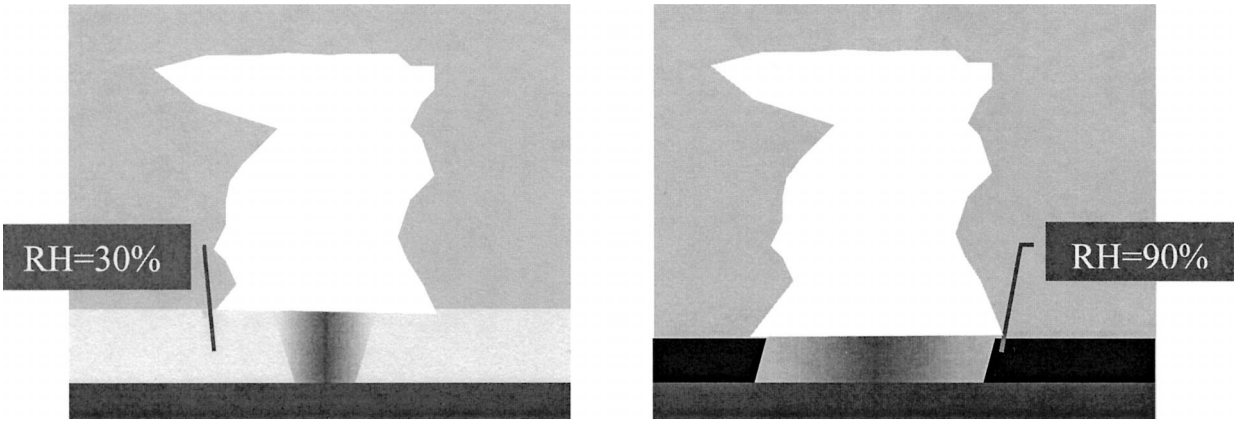

FIG. 7. Environments with relatively (left) dry and (right) moist low levels. The boundary layer with the more moist environment would likely exhibit a lower cloud base and a broader precipitation footprint.

A schematic diagram of the physical effect of surface-to-LCL relative humidity is shown in Fig. 7. The LCL represents the height to which air originating near the surface must rise to condense and to form cloud material, thus making it the assumed level of the cloud base. The layer defined from the surface to the LCL is usually the storm moisture-intake depth and is where precipitation leaving the cloud base becomes susceptible to evaporation. As low-level relative humidity is reduced, more of the precipitation leaving the cloud evaporates before reaching the ground, decreasing the numerator of the PE definition. As the sub-cloud-base relative humidity increases, PE increases because of limited evaporation below the cloud base.

Figure 8 depicts the environmental settings when CIN affects PE. CIN is a measure of the energy required to overcome a negatively buoyant layer and produce upward vertical motion. In this case, CIN is calculated by lifting a parcel of air that has the characteristics of the lowest 100 hPa of the atmosphere. As CIN decreases (Fig. 8, left) and upward vertical motion is easier to achieve and maintain, PE increases because of the increasing ability to lift, condense, and aggregate water vapor into precipitation particles large enough to fall to the ground. When CIN is maximized and the atmosphere is said to be ''capped,'' more energy must be expended to create an updraft. If CIN is nonexistent over a region, then numerous convective updrafts may form and exhaust the instability in the layer above before organized convection can begin. The inverse correlation of decreasing CIN to increasing PE suggests that a stronger cap may lead to fewer, more isolated cells that will be more vulnerable to the effects of entrainment, thus reducing the likelihood that convective cells will live long enough to form into an organized convective system. Last, we note also the positive correlation ($r = 0.54$) between decreasing CIN and decreasing cloud-base height (which progressively prohibits evaporation in the subcloud layer).

Bulk cloud shear is depicted in Fig. 9 and is the difference in the speed of the wind over the depth of the warm cloud. It is related to PE inversely, and so for increasing shear, PE decreases. As the shear increases, a cloud will be more tilted over, allowing for more contact with drier environmental air, helping to decrease PE by aiding evaporation of potential precipitation. This last correlation agrees in sign with that of Marwitz (1972). Stronger winds aloft are also known to advect cirrus mass downwind, from which precipitation may be falling. Not only can cirrus anvils alter the three-dimensional moisture field around an MCS, but they introduce shadows that can alter the thermodynamic profile around the system (Markowski et al. 1998).

To support statistically the ''robust inverse relationship'' discussed by Lamb (2001), the data points from the Marwitz (1972) curve shown in Lamb (2001) are estimated and processed to arrive at a statistical regression. Results of the quadratically fitted curve based on the Marwitz (1972) values are presented in Fig. 10. To compare results of the current research, a quadratically fitted curve is also created for the cases studied herein, as seen in Fig. 11. The results of the Marwitz (1972) statistical analysis show a quadratic relationship that accounts for 87.4% of the variance of PE (Fig. 10), whereas current values support a quadratic relationship accounting for 16.6% of the variance of PE (Fig. 11). The range of PE values in the current work may not allow for such a strong relationship to be found, although the data sample in the Marwitz (1972) analysis was of similar size. The most likely cause of the disparity between the Marwitz analysis and that presented here is the difference in approaches to the calculation of PE. Most of the studies whose values compose the Marwitz analysis are based upon the flux approach to calculating PE. In addition, a number of those values were based upon aircraft data, and some were calculated for individual convective elements. The current study attempts to address the bulk PE of an entire MCS over the course of its life cycle.

Some variables that would seem to have strong phys-

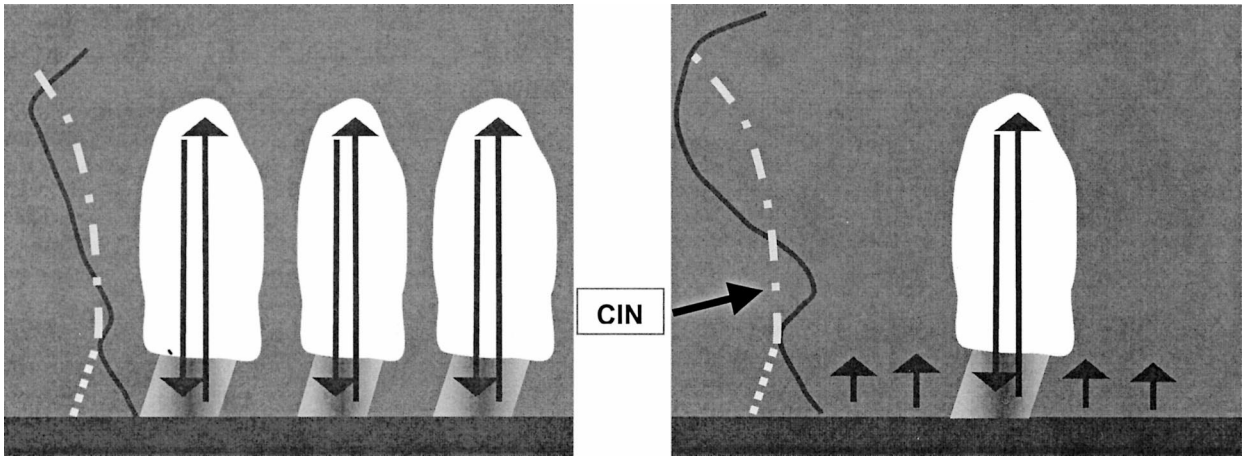

FIG. 8. Environments with (left) little to no CIN and (right) significant CIN, as depicted by a sample sounding profile (temperature is dark, solid; moist adiabat is light, dash–dot). Arrows represent the effectiveness with which updrafts break the cap. On the right, an increase in CIN permits fewer, more isolated updrafts that allow more evaporation or entrainment than the more numerous cells and updrafts found with lower-CIN cases.

ical reasons to influence PE do not show significant correlation. One of those is CAPE. Fankhauser (1988) also believed that CAPE should correlate with PE but found no such relationship. It would seem that the potential for strong updrafts could enhance PE, but the correlations show that it is the amount of energy to be overcome to create and maintain updrafts that affects PE more. One possible explanation for why this relationship exists lies in the fact that when CIN is minimized, even a modest amount of CAPE will produce updrafts strong enough to collect precipitation particles effectively, but, even for large CAPE, CIN can also be large and updrafts may never form, making CIN the dominant variable. It has also been suggested that very large CAPE values may lower PE, because the strong updraft afforded by a large CAPE would eject too much condensate out of the anvil. If this were true, then one might expect a curvilinear relationship in which PE and CAPE are positively correlated up to an ''optimal'' value and then become negatively correlated, with PE decreasing as the CAPE continues to increase. The current dataset failed to exhibit such behavior.

Other variables that do not correlate well with PE include the PW. This at first appears to be counterintuitive, but note that although adding moisture to the atmosphere should increase precipitation, it does not necessarily follow that PE will be higher. Thus, increasing PW does not necessarily increase PE. Indeed, high PW is a necessary but not sufficient condition for heavy precipitation; a mechanism to lift the moist air parcels and condense out their moisture is also required. Another variable that does not correlate well with PE is the warm cloud depth, which is measured from the cloud base up to where core cloud temperatures reach freezing

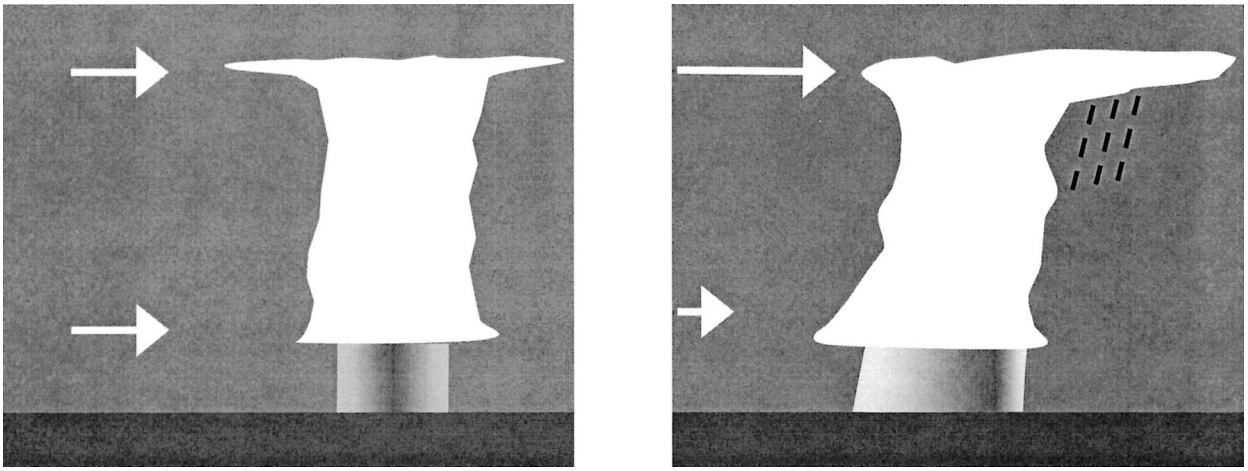

FIG. 9. Environments with (left) little to no cloud shear and (right) significant cloud shear. The no-shear case allows for a more erect cumulus tower, less entrainment of dry ambient air, and, thus, more precipitation falling over a smaller area.

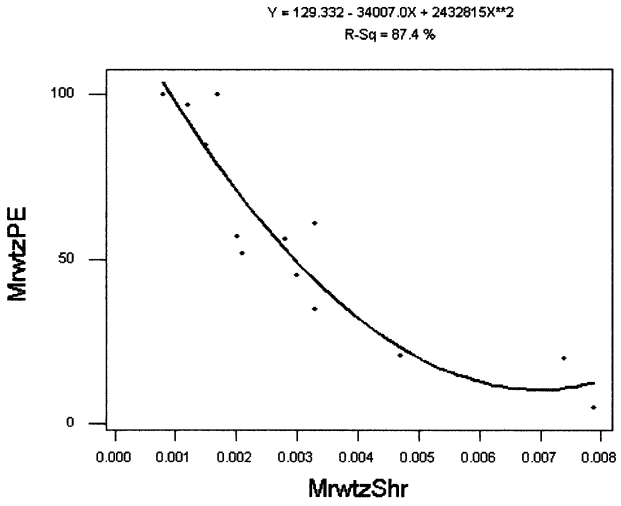

FIG. 10. Statistical analysis of the data from the Marwitz (1972) cloud-shear-vs-PE curve.

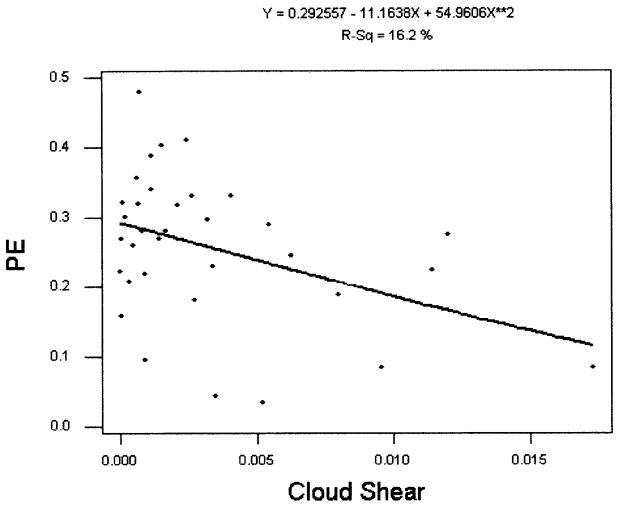

FIG. 11. As in Fig. 6, but including a quadratically fitted regression curve.

and is important because it defines the layer of the cloud in which collision–coalescence is the dominant process for precipitation droplet growth. Warm cloud depth might have correlated better with PE if our dataset had contained a greater variety of depths. Considering that the range of calculated warm cloud depths is small in the summertime, PE studies that incorporate year-round calculations (perhaps in the southern United States) would have better opportunity to capture a systematic relationship. In the case of heavy precipitation, the warm cloud depth is another instance in which large depths are necessary but not sufficient for creating excessive rainfall. Last, the relative humidity surrounding the warm cloud depth would seem also to influence PE, because very dry cloud surroundings would tend to evaporate cloud material from the sides and decrease the moisture available to create precipitation. However, the range of extracloud humidity is small in the summer, making a relationship difficult to determine. This is especially significant because Newton (1966) postulated that the entrainment of drier environmental air into the cloud was the cause of the decrease of PE with increasing shear. Although this relationship may well be true for the individual cumulonimbus, such does not appear to be the case for the large collections of cumulonimbi manifested by an MCS. Also the low-level kinetic energy (Fankhauser 1988), here based upon the winds at 950 hPa, failed to correlate significantly with PE.

5. Conclusions

A predictive relationship between warm-season Midwestern MCS PE and GOES sounding profiles is established. To achieve this goal, a PE calculation method is presented that is based on a climatological PE definition. By decreasing the time step to 6-h precipitation for the Sellers PE numerator and corresponding precipitable water for the denominator, the definition captures features such as MCS that have timescales of hours. When compared with the work of other researchers, our PE values are similar to those previously reported, though our values were lower than those found by earlier researchers, suggesting the possibility of a systematic error.

Using these PE values in conjunction with environmental parameters derived from GOES soundings representative of air available to the MCS, statistical analysis is performed on the data. Individual correlations show both direct and inverse relationships, and two of the best correlates provide statistical support for previously hypothesized relationships. The single correlations affirm that PE is controlled by certain environmental factors, namely, vertical wind shear, sub-cloud-base moisture, and convective inhibition. The implications of these statistically significant relationships reach into the realm of forecasting, providing a basis for advanced prediction capability.

Other interesting results were found with respect to the work of previous authors. The shear curve of Marwitz (1972) shows a negative correlation, the statistical significance of which is quantified here. Our statistical analysis shows the same negative correlation between wind shear and PE, but it is not so dramatic. With more data points from more years of calculation, perhaps the high and low end of the PE scale could be better filled with shear values to support the Marwitz (1972) curve. Newton's (1966) contention that the relative humidity around a cloud would act to increase or decrease PE was not supported by the single correlations, but that fact could be attributed to a small dataset with small ranges or to the size of MCSs. Most surprising was the relatively strong negative correlation with PE of CIN calculated for a parcel originating in the lowest 100 hPa. Previous authors had postulated the importance of

CAPE yet had not supported it; we also failed to establish a statistical relationship between PE and CAPE. This work shows a much stronger and statistically significant correlation with CIN.

Acknowledgments. The authors thank Drs. Adnan Akyüz, Neil Fox, and Anthony Lupo and Mr. Jaime Daniels for numerous conversations and comments regarding precipitation systems that improved this work. Messrs. Michael Baker and Brett McDonald of the National Centers for Environmental Prediction have our sincere thanks for making available the radar-derived precipitation data that were necessary for the calculation of PE. Brian Pettegrew of Central Methodist College, and Mark Gall, Eric Kelsey, Amy Maddox, and Derrick Weitlich of the University of Missouri-Columbia have our gratitude for assisting with this research. This work is supported by NOAA/NESDIS/ORA Award NA06EC0202.

REFERENCES

Auer, A. H., and J. D. Marwitz, 1968: Estimates of air and moisture flux into hailstorms on the High Plains. *J. Appl. Meteor.,* **7,** 196–198.

Braham, R. R., 1952: The water and energy budgets of the thunderstorm and their relation to thunderstorm development. *J. Meteor.,* **9,** 227–242.

Caracena, F., R. A. Maddox, L. R. Hoxit, and C. F. Chappell, 1979: Mesoanalysis of the Big Thompson storm. *Mon. Wea. Rev.,* **107,** 1–17.

Carbone, R. E., 1982: A severe frontal rainband. Part I: Stormwide hydrodynamic structure. *J. Atmos. Sci.,* **39,** 258–279.

Chalon, J.-P., J. C. Fankhauser, and P. J. Eccles, 1976: Structure of an evolving hailstorm. Part I: General characteristics and cellular structure. *Mon. Wea. Rev.,* **104,** 564–575.

Chisholm, A. J., 1968: Observations by 10-cm radar of an Alberta hailstorm in a sheared environment. Preprints, *13th Radar Meteorology Conf.,* Montreal, QC, Canada, Amer. Meteor. Soc., 82–87.

——, 1970: Alberta hailstorms: A radar study and model. Ph.D. thesis, McGill University, 237 pp.

Chong, M., and D. Hauser, 1989: A tropical squall line observed during the COPT 81 experiment in West Africa. Part II: Water budget. *Mon. Wea. Rev.,* **117,** 728–744.

Cotton, W. R., M.-S. Lin, R. L. McAnelly, and C. J. Tremback, 1989: A composite model of mesoscale convective complexes. *Mon. Wea. Rev.,* **117,** 765–783.

Dostalek, J. F., and T. J. Schmit, 2001: Total precipitable water measurements from GOES sounder derived product imagery. *Wea. Forecasting,* **16,** 573–587.

Doswell, C. A., H. E. Brooks, and R. A. Maddox, 1996: Flash flood forecasting: An ingredients-based methodology. *Wea. Forecasting,* **11,** 560–581.

Fankhauser, J. C., 1966: Some physical and dynamical aspects of a singular cumulonimbus observed by instrumented aircraft and radar. Preprints, *12th Conf. on Radar Meteorology,* Norman, OK, Amer. Meteor. Soc., 405–413.

——, 1988: Estimates of thunderstorm precipitation efficiency from field measurements in CCOPE. *Mon. Wea. Rev.,* **116,** 663–684.

Ferrier, B. S., J. Simpson, and W. K. Tao, 1996: Factors responsible for precipitation efficiencies in midlatitude and tropical squall simulations. *Mon. Wea. Rev.,* **124,** 2100–2125.

Foote, G. B., and J. C. Fankhauser, 1973: Airflow and moisture budget beneath a northeast Colorado hailstorm. *J. Appl. Meteor.,* **12,** 1330–1353.

Fulton, R. A., J. P. Breidenbach, D. J. Seo, and D. A. Miller, 1998: The WSR-88D rainfall algorithm. *Wea. Forecasting,* **13,** 377–395.

Gamache, J. F., and R. A. Houze, 1983: Water budget of a mesoscale convective system in the Tropics. *J. Atmos. Sci.,* **40,** 1835–1850.

Hanesiak, J. M., R. E. Stewart, K. K. Szeto, D. R. Hudak, and H. G. Leighton, 1997: The structure, water budget, and radiational features of a high-latitude warm front. *J. Atmos. Sci.,* **54,** 1553–1573.

Hartzell, C. L., 1969: Case study of a traveling hailstorm. M.S. thesis, South Dakota School of Mines and Technology, 72 pp.

Heymsfield, G. M., and S. Schotz, 1985: Structure and evolution of a severe squall line over Oklahoma. *Mon. Wea. Rev.,* **113,** 1563–1589.

Hindman, E. E., P. J. DeMott, and L. O. Grant, 1981: Precipitation efficiency studies of Colorado winter storms and storm-stages. *Extended Abstracts, Eighth Conf. on Inadvertent and Planned Weather Modification,* Reno, NV, Amer. Meteor. Soc., 56–57.

Hobbs, P. V., T. J. Matejka, P. H. Herzegh, J. D. Locatelli, and R. A. Houze, 1980: The mesoscale and microscale structure and organization of clouds and precipitation in midlatutude cyclones. I: A case study of a cold front. *J. Atmos. Sci.,* **37,** 568–596.

Houze, R. A., J. D. Locatelli, and P. V. Hobbs, 1976: Dynamics and cloud microphysics of the rainbands in an occluded frontal system. *J. Atmos. Sci.,* **33,** 1921–1936.

Kadin, C., and S. J. Kusselson, 2000: Use of GOES sounder data to forecast a winter convective heavy rain/flash flood event in the Mississippi Valley. *Natl. Wea. Dig.,* **24,** 27–37.

Lamb, D., 2001: Rain production in convective storms. *Severe Convective Storms, Meteor. Monogr.,* No. 50, Amer. Meteor. Soc., 299–321.

Li, X., C.-H. Sui, and K.-M. Lau, 2002: Precipitation efficiency in the tropical deep convective regime: A 2-D cloud resolving modeling study. *J. Meteor. Soc. Japan,* **80,** 205–212.

Lipps, F. B., and R. S. Hemler, 1986: Numerical simulation of deep tropical convection associated with large-scale convergence. *J. Atmos. Sci.,* **43,** 1796–1816.

Markowski, P. M., E. N. Rasmussen, J. M. Straka, and D. C. Dowell, 1998: Observations of low-level baroclinicity generated by anvil shadows. *Mon. Wea. Rev.,* **126,** 2942–2958.

Marwitz, J. D., 1972: Precipitation efficiency of thunderstorms on the High Plains. *J. Res. Atmos.,* **6,** 367–370.

McBean, G. A., and R. E. Stewart, 1991: Structure of a frontal system over the northeast Pacific Ocean. *Mon. Wea. Rev.,* **119,** 997–1013.

Menzel, W. P., and J. F. W. Purdom, 1994: Introducing GOES-I: The first of a new generation of geostationary operational environmental satellites. *Bull. Amer. Meteor. Soc.,* **75,** 757–781.

——, F. C. Holt, T. J. Schmit, R. M. Aune, A. J. Schreiner, G. S. Wade, and D. G. Gray, 1998: Application of *GOES-8/9* soundings to weather forecasting and nowcasting. *Bull. Amer. Meteor. Soc.,* **79,** 2059–2077.

Moore, J. T., and J. P. Pino, 1990: An interactive method for estimating maximum hailstone size from forecast soundings. *Wea. Forecasting,* **5,** 508–525.

Newton, C. W., 1966: Circulations in large sheared cumulonimbus. *Tellus,* **18,** 699–712.

Rauber, R. M., N. F. Laird, and H. T. Ochs, 1996: Precipitation efficiency of trade wind clouds over the north central tropical Pacific Ocean. *J. Geophys. Res.,* **101,** 26 247–26 253.

Ryan, B. F., K. J. Wilson, and E. J. Zipser, 1989: Modification of the thermodynamic structure of the lower troposphere by the evaporation of precipitation ahead of a cold front. *Mon. Wea. Rev.,* **117,** 138–153.

Scofield, R., G. Vicente, and M. Hodges, 2000: The use of water vapor for detecting environments that lead to convectively produced heavy precipitation and flash floods. NOAA Tech. Rep. NESDIS 99, 64 pp.

Sellers, W. D., 1965: *Physical Climatology.* The University of Chicago Press, 272 pp.

Szeto, K. K., R. E. Stewart, and J. M. Hanesiak, 1997: High-latitude cold season frontal cloud systems and their precipitation efficiency. *Tellus,* **49A,** 439–454.

Thompson, R. L., and R. Edwards, 2000: A comparison of Rapid Update Cycle 2 (RUC-2) Model soundings with observed soundings in supercell environments. Preprints, *20th Conf. on Severe Local Storms,* Orlando, FL, Amer. Meteor. Soc., 551–554.